Damage Detection in Tensegrity using Interacting Particle-Ensemble Kalman Filter

Neha Aswal, Subhamoy Sen, Laurent Mevel

Damage Detection in Tensegrity using Interacting Particle-Ensemble Kalman Filter

Neha Aswal[1 [0000−0003−3923−3592]], Subhamoy Sen[1 [0000−0001−8021−6693]], and Laurent Mevel[2 [0000−0001−8913−7393]]

[1] Indian Institute of Technology Mandi, Himachal Pradesh, India
[2] Univ. Gustave Eiffel, Inria, Cosys-SII, I4S, Campus de Beaulieu, France
nehaaswal96@gmail.com, subhamoy@iitmandi.ac.in,laurent.mevel@inria.fr

Abstract. Tensegrity structures form a special class of truss with dedicated cables and bars, that take tension and compression, respectively. To ensure equilibrium, the tensegrity members are required to be prestressed. Over prolonged usage, the cables may lose their prestress while bars may buckle, affecting the structural stiffness as well as its dynamic properties. The stiffness of tensegrities also vary with the load even in the absence of damage. This can potentially mask the effect of damage leading to a false impression of tensegrity health. This poses a major challenge in tensegrity health monitoring especially when the load is stochastic and unknown.

Present study develops a vibration based output-only time-domain approach for monitoring the health of any tensegrity in the presence of uncertainties due to ambient force and measurement noise. An Interacting Particle Ensemble Kalman Filter (IPEnKF) has been used that can efficiently monitor tensegrity health from contaminated response data. IPEnKF combines a bank of Ensemble Kalman Filters to estimate response states while running within a Particle Filter envelop that estimates a set of location based health parameters. Further to make damage detection cheaper, strain responses are used as measurements. The efficiency of the proposed methodology has been demonstrated using numerical experiments performed on a simplex tensegrity.

Keywords: Tensegrity · Structural Health Monitoring · Interacting Particle Ensemble Kalman Filter · Damage Detection

1 Introduction

Coined by Buckminster Fuller, the term *tensegrity* is a combination of the words - *tension* and *integrity*. As the name suggests, these structures derive their integrity from the prestress present in their members. From being introduced as a simple yet elegant piece of art by Snelson to being utilised in various complex and state of the art engineering structures like masts, stadium roofs, bridges, space and aerospace

structures, tensegrity has come a long way in less than a century. Tensegrities are light-weight and help creating large column-free spaces. Many researchers have developed various design methodologies for complex tensegrities that are statically stable and can be constructed into reality. Tensegrities are self-stiffening structures. They can modify their stiffnesses through morphing their shape in order to carry any external load. Consequently, the vibrational response of the structure [1] gets affected by the external loading. It should therefore be noted that, stiffness alteration due to member prestress modification induced by force variability does not imply a damage in the structure.

Hence, to identify a possible structural anomaly in tensegrity, it is important to have an Structural Health Monitoring (SHM) approach that takes the inherent nature of tensegrity [2] into account, yet very less literature is available on this. Bhalla et. al. [3] successfully assessed the damage existing in tensegrity using dynamic strain measurements. Sychterz and Smith [4] compared three methods to detect damage in tensegrity, namely, frequency analysis, error-domain model falsification (EDMF) using node position measurement and moving-window principal component analysis (MWPCA) using strain measurements. It was observed that the natural frequencies and the mode shapes cannot be used to detect and localize the damage in a tensegrity. The complexities involved with tensegrity mode shapes do not support damage identification. EDMF tends to become costly when tracking positions at submillimeter resolution and the results are sensitive to the amount of ambient uncertainty. MWPCA has an advantage as it uses inexpensive strain gauges and is efficient with noisy signal with high signal to noise ratio (SNR) but fails at low SNR levels.

Evidently, most of the works pertaining to tensegrity health monitoring is defined for deterministic scenarios. Nevertheless, for a real one, uncertainties arise during modelling error, ambient forcing and noise in the measurement which cannot be accounted for in a deterministic approach. In order to propose a practical SHM approach aimed to monitor real life tensegrities, it is necessary to incorporate the effects of uncertainties originating from unavoidable model inaccuracies, sensor noises and unknown external disturbances.

Bayesian filtering has proved its efficiency in detecting damage in structures in presence of uncertainties. Bayesian filtering approaches define the structural dynamics using a set of unobserved variables-termed as "states". The state dynamics and their impact on the measured responses are further defined using two separate probabilistic models, namely, process and measurement models/equations which individually account for uncertainties arising from ambient forcing and sensor noises. The inherent self-stiffening property of tensegrities [2] can be modelled by considering the geometric non-linearity in the dynamic model. This physical space dynamic model subjected to a stochastic input forcing is further transformed into a discrete time state space model to facilitate the estimation of the system states. A set of location based health parameters, $\theta_{\mathbf{k}}$, to monitor the tensegrity health in terms of stiffness

deterioration, is further added to the state definition as parameter states alongside the regular system states.

Evidently, the process equation is non-linear. In addition, the mapping of the mentioned health parameters to the corresponding measured responses is also non-linear. Handling these non-linearities simultaneously poses a major challenge in tensegrity SHM. Using an Interacting filtering technique can be a reliable option [5] for such system health estimation problems. This paper attempts to employ an Interacting Particle Ensemble Kalman Filtering (IPEnKF) strategy to estimate health of tensegrity in presence of process and measurement uncertainties. The major benefit with this approach is that the computational efficiency can easily be enhanced by exploiting the flexibility of parallelization of the complete computation, allowing to target a prompt detection of damage.

2 Geometric Non-linear Finite Element Model

Non-linearity in a structure may arise due to geometric (large deformations, etc.), material (plasticity, etc.) or boundary (contact) non-linearity. Geometric non-linearity is only considered in this study since strain-displacement relation, in a tensegrity, is prominently non-linear. Since tensegrity can typically be classified as a special case of truss, its finite element model (FEM) can be considered with a typical bar element defined with natural discretization [6].

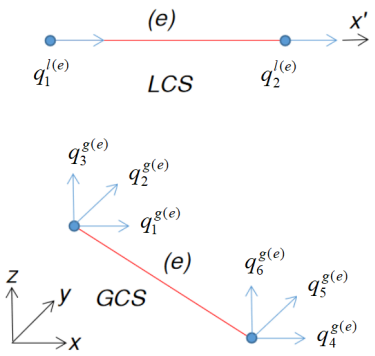

Fig. 1: LCS and GCS for bar element type

The transformation from global coordinate system (GCS) to local coordinate system (LCS) is performed using the transformation matrix, $\mathbf{T}$ as,

$$\mathbf{q}_k^l = \mathbf{T}\mathbf{q}_k^g \tag{1}$$

with, $\mathbf{T} = \begin{bmatrix} cos\theta_x & cos\theta_y & cos\theta_z & 0 & 0 & 0 \\ 0 & 0 & 0 & cos\theta_x & cos\theta_y & cos\theta_z \end{bmatrix}$, $\mathbf{q}_k^l = \{q_1^l \quad q_2^l\}_k^T$ and $\mathbf{q}_k^g = \{q_1^g \quad q_2^g \quad q_3^g \quad q_4^g \quad q_5^g \quad q_6^g\}_k^T$. Subscript k denotes the time step at which the stiffness is being defined. The deformation at any point in the element can further be defined using its nodal displacements and shape functions N_1 and N_2 as,

$$\mathbf{u}_k^* = [N_1 \quad N_2]\mathbf{q}_k^l \tag{2}$$

where $N_1 = (1-r)/2$ and $N_2 = (1+r)/2$ are the shape functions defined in the natural coordinate system with r being the natural variable defined within the range $-1 \leq r \leq 1$. The strain field can further be obtained differentiating the displacement field including second order expansion as,

$$\varepsilon_k^{(e)} = \frac{\partial \mathbf{u}_k^*}{\partial x} + \frac{1}{2}\left(\frac{\partial \mathbf{u}_k^*}{\partial x}\right)^2 \tag{3}$$

which leads to the following expansion including the linear and non-linear parts of the strain as,

$$\varepsilon_k^{(e)} = \{\mathbf{B}_L \mathbf{q}_k^l\}_{linear} + \{\mathbf{B}_{NL}(\mathbf{q}_k^l)\mathbf{q}_k^l\}_{non-linear} \tag{4}$$

where $\mathbf{B}_L = \left[\frac{\partial N_1}{\partial x} \; \frac{\partial N_2}{\partial x}\right]$ and $\mathbf{B}_{NL}(\mathbf{q}_k^l) = \frac{1}{2}{\mathbf{q}_k^l}^T \begin{bmatrix} \partial N_1/\partial x \\ \partial N_2/\partial x \end{bmatrix} \left[\frac{\partial N_1}{\partial x} \; \frac{\partial N_2}{\partial x}\right]$ are linear and non-linear strain-displacement matrices, respectively.

Employing the principle of virtual work, the element stiffness matrix can be obtained by equating the work done by the internal forces to the virtual work done by the external forces.

$$\int_{V^{(e)}} \varepsilon_k^{(e)} \sigma_k^{(e)} dV = \{\delta \mathbf{q}_k^l\}^T \mathbf{F}_k^{(e)} \tag{5}$$

with $\sigma_k^{(e)}$ being the member stress that can be obtained from the constitutive relation as $\sigma_k^{(e)} = \mathbf{E}^{(e)} \varepsilon_k^{(e)}$ with $\mathbf{E}^{(e)}$ being the constitutive matrix. With this, Eq. (5) can be expanded as,

$$\int_{V^{(e)}} \delta {\mathbf{q}_k^g}^T \mathbf{T}^T \mathbf{B}_k^T \mathbf{E}^{(e)} \mathbf{B}_k \mathbf{T} \delta \mathbf{q}_k^g dV = \{\delta \mathbf{q}_k^g\}^T \mathbf{F}_k^{(e)} \tag{6}$$

with $\mathbf{B}_k = \mathbf{B}_L + \mathbf{B}_{NL}(\mathbf{q}_k^l)$. Imposing the non-trivial solution condition, $\{\partial \mathbf{q}_k^l\} \neq 0$ and further comparing with $\mathbf{F}_k^{(e)} = \mathbf{K}_k^{(e)} \delta \mathbf{q}_k^g$, the element stiffness matrix in the natural coordinate system can be obtained as,

$$\mathbf{K}_k^{(e)} = \mathbf{E}^{(e)} A^{(e)} \int_{-1}^{1} \mathbf{T}^T \mathbf{B}_k^T \mathbf{B}_k \mathbf{T} \frac{l^{(e)}}{2} dr \tag{7}$$

assuming a uniform cross section $\mathbf{A}^{(e)}$ over the entire length $l^{(e)}$ of the element e. The Gauss-Quadrature method has further been applied to find the numerical integration

for the above integral ($ng = 1$). Assembling all the element stiffness matrices and applying the natural boundary conditions, one can get the global stiffness matrix $\mathbf{K}_k$. Similarly, the mass matrix $\mathbf{M}$ can be obtained by following the consistent mass matrix assumption.

2.1 Non-linear Response from Newmark-beta

Due to its superior accuracy, Newmark-beta is one of the popular methods to find the response of the non-linear systems. The method solves an incremental equilibrium equation (see Eq. (8)) to find non-linear structural response variables , i.e., $\ddot{\mathbf{u}}_k, \dot{\mathbf{u}}_k$ and $\mathbf{u}_k$, of the following governing differential equation,

$$\mathbf{M}\Delta\ddot{\mathbf{u}}_k + \mathbf{C}_k(\mathbf{u}_k)\Delta\dot{\mathbf{u}}_k + \mathbf{K}_k(\mathbf{u}_k)\Delta\mathbf{u}_k = \Delta\mathbf{P}_k \tag{8}$$

where, $\ddot{\mathbf{u}}_{k_{(n\times 1)}}, \dot{\mathbf{u}}_{k_{(n\times 1)}}$ and $\mathbf{u}_{k_{(n\times 1)}}$ are the acceleration, velocity and displacement responses, respectively and the Δ operator signifies the corresponding increment over each time step. $\mathbf{M}_{(n\times n)}$ is the time invariant global mass and $\mathbf{C}_{k_{(n\times n)}}$ and $\mathbf{K}_{k_{(n\times n)}}$ are the time dependent damping and stiffness matrices of the structure, respectively. The time dependence of $\mathbf{K}_k$ originates from its dependence on the displacement response $\mathbf{u}_k$. With Rayleigh damping assumption, $\mathbf{C}_k$ being a function of $\mathbf{K}_k$ is also time dependent. $\mathbf{P}_{k_{(n\times 1)}}$ is the external force acting on the structure.

Clearly, the above dynamics is an implicit equation which requires an iterative solution at each step. However, in the context of tensegrity SHM, the same equation can be redefined using an explicit formulation with Newmark-beta explicit integration scheme without losing much on the precision yet achieving promptness in detection. Newmark-beta is a well established method and for the sake of brevity, it is not discussed here. Details of this method can be found in [7]. The method shows an unconditional stability for $\gamma = 0.5$ and $\beta = 0.25$ (average constant acceleration assumption), hence these values are utilised in this study.

3 State space formulation for system dynamics

Bayesian filtering employs a process equation to define the system dynamics in terms of dynamics of a set of unobserved variable, named as states. To estimate the time varying nature of the system due to damage, a set of location based health parameters, $\theta_{\mathbf{k}}$, are additionally defined as parameter states. These health parameters monitor the residual elasticity after damage within a range of $[0, 1]$ in which 0 and 1 mean complete and no damage, respectively. While the system states are estimated using a bank of EnKF (Ensemble Kalman Filter), the parameter states are estimated through an envelop PF (Particle Filter).

Within EnKF, the system dynamics is defined with displacement, velocity and acceleration responses in the state vector, i.e. $\mathbf{X}_k = \{\mathbf{u}_k \quad \dot{\mathbf{u}}_k \quad \ddot{\mathbf{u}}_k\}^T$. The previously detailed non-linear FEM of tensegrity is further employed to propagate these system states in time. Prior to this, the tensegrity stiffness needs to be re-calibrated considering the current nodal displacement that causes a change in the prestress. Integrated using the Guass-Quadrature method, Eq. (7) is discretized to find the discrete elemental stiffness matrix with $\mathbf{B}_{k-1}$ re-calibrated as $\mathbf{B}_k$ using the current nodal displacements $\mathbf{u}_{k-1}$. All the elemental stiffness matrices are further assembled to obtained the global stiffness matrix $\mathbf{K}_k$. Next, the system states are forwarded in time using the Newmark-beta integration scheme.

$$\mathbf{X}_k = f(\mathbf{X}_{k-1}, \mathbf{K}_k, \mathbf{M}, dt, \mathbf{P}_k) + \mathbf{v}_k \tag{9}$$

where f denotes the intrinsic calculations involved in Newark-beta integration scheme. dt denotes the time step for which the simulation is performed. $\mathbf{P}_k$ is the stochastic ambient force acting on the structure modelled as a white Gaussian noise (WGN) of distribution $\mathbb{N}(0, \mathbf{Q}_k^P)$. [1] The process noise $\mathbf{v}_k$ accounts for the unavoidable inaccuracies in the prediction model $f(\bullet)$ and can be modelled as WGN of distribution $\mathbb{N}(0, \mathbf{Q}_k)$.

Next, the unobserved response states are mapped to the corresponding strain fields in several members using the non-linear strain measurement mapping equation. The dependence of the strain-displacement matrix $\mathbf{B}_k$ on the displacement $\mathbf{u}_k^l$ can be demonstrated using the notation $\mathbf{B}(\mathbf{X}_k)$ since $\mathbf{u}_k$ is a subset of $\mathbf{X}_k$. The measurement equation can then be obtained from Eq. (4) by incorporating the partial measurement information and the sensor noises as,

$$\mathbf{y}_k = \mathbf{H}\mathbf{B}(\mathbf{X}_k)\mathbf{T}\mathbf{X}_k + \mathbf{w}_k \tag{10}$$

where $\mathbf{H}$ is the selection matrix that defines which of the member strains are measured. $\mathbf{w}_k$ accounts for measurement noises arising from the sensors modeled using WGN model of distribution $\mathbb{N}(0, \mathbf{R}_k)$.

4 System estimation using IPEnKF algorithm

The system states are estimated using an IPEnKF algorithm which is a modification of the Interacting Particle-kalman Filter (IPKF) algorithm [8]. With IPEnKF, the response states are estimated using a nested EnKF instead of KF to enable handling the non-linear systems, while an enveloping PF estimates the parameter $\theta_{\mathbf{k}}$. All of the filtering steps are briefly described in the following. The details can be found in the article [8].

[1] $A + B\mathbb{N}(\mu; \sigma)$ means $A + Bz$ where z follows $\mathbb{N}(\mu; \sigma)$

4.1 Envelop parameter filter - PF

In order to avoid an explicit analytical integration over the entire parameter space, $\theta_{\mathbf{k}}$, a particle approximation of this integration is approached with PF that propagates the parametric uncertainty thorough a cloud of N_p independent particles $\Xi_k = [\xi_k^1, \xi_k^2, \cdots, \xi_k^{N_p}]$. At each time step, the particle distribution gets updated depending on their likelihood against measured data and thus no assumption is needed on their distribution apriori.

Within the envelop PF, the particle representations of parameter estimates evolve assuming a Gaussian perturbation around the current estimate ξ_{k-1}^j as,

$$\xi_k^j = \xi_{k-1}^j + \mathbb{N}(\delta\xi_k; \sigma_k^\xi) \tag{11}$$

where a Gaussian blurring is performed on ξ_{k-1}^j with a shift $\delta\xi_k$ and a spread of σ_k^ξ. For each of the particles, the corresponding stiffness matrix, i.e., $\mathbf{K}_{k-1|k-1}^j$, is first calculated and supplied to each of the EnKF candidates.

4.2 Nested state filter - EnKF

In the nested EnKF, N_e sets of state ensembles for each j^{th} parameter particle are propagated through the system state propagation model (see Eq. (9)). However, since the tensegrities are functions of nodal displacements, the supplied stiffness matrix $\mathbf{K}_{k-1|k-1}^j$ has to be further modified based on the current estimate of nodal displacement responses ${\mathbf{q}_{k-1|k-1}^g}^{i,j}$ which is a subset of the state estimate $X_{k-1|k-1}^{i,j}$ pertinent to j^{th} particle and i^{th} ensemble. Eq. (7) can be employed and can be expressed as,

$$\mathbf{K}_{k|k-1}^{i,j} = m(\mathbf{K}_{k-1|k-1}^j, \mathbf{X}_{k-1|k-1}^{i,j}) \tag{12}$$

where $m(\bullet)$ is the stiffness calibration function detailed in Eq. (7). With the modified stiffness matrix $\mathbf{K}_{k|k-1}^{i,j}$ and a realization for the ambient forcing, $\mathbf{P}_k^{i,j}$, drawn from a known statistic (say $\mathcal{N}(0, \mathbf{Q}^f)$), the prior state estimates $\mathbf{X}_{k-1|k-1}^{i,j}$ are propagated to the next time step as $\mathbf{X}_{k|k-1}^{i,j}$,

$$\mathbf{X}_{k|k-1}^{i,j} = f(\mathbf{X}_{k-1|k-1}^{i,j}, \mathbf{K}_{k|k-1}^{i,j}, \mathbf{M}, dt, \mathbf{P}_k^{i,j}) + \mathbf{v}_k^{i,j} \tag{13}$$

The measurement function described in Eq. (10) is further employed to map each of the ensembles to the corresponding measurement prediction, $\mathbf{y}_{k|k-1}^{i,j}$ from which innovation, $\epsilon_{k|k-1}^{i,j}$, for each ensemble, can be obtained from the corresponding real measurement $\mathbf{y}_k$. Next, the ensemble mean estimates for the propagated states ($\mathbf{X}_{k|k-1}^j$)

and predicted measurements ($\mathbf{y}^j_{k|k-1}$) are obtained as means of corresponding entities for all ensembles. Cross-covariance between state and measurement prediction $C^{j,XY}_k$ and the measurement prediction covariance $C^{j,YY}_k$ can further be computed following [9]. The innovation error covariance, $\mathbf{S}^j_k$ and EnKF gain, $\mathbf{G}^j_k$, are then obtained as $\mathbf{S}^j_k = C^{j,\mathbf{YY}}_k + \mathbf{R}_k$ and $\mathbf{G}^j_k = C^{j,\mathbf{XY}}_k (\mathbf{S}^j_k)^{-1}$. With this gain, the state ensembles are updated as,

$$\mathbf{X}^{i,j}_{k|k} = \mathbf{X}^{i,j}_{k|k-1} + \mathbf{G}^j_k \epsilon^{i,j}_{k|k-1} \tag{14}$$

4.3 Particle approximation

Likelihood of each particle, i.e. $\mathcal{L}(\xi^j_k)$, is further calculated based on the innovation mean $\epsilon^j_{k|k-1}$ and co-variance, $\mathbf{S}^j_k$, of all the ensemble simulations running within it. The normalized weight for each j^{th} particle is further updated as,

$$w(\xi^j_k) = \frac{w(\xi^j_{k-1})\mathcal{L}(\xi^j_k)}{\sum_{j=1}^{N} w(\xi^j_{k-1})\mathcal{L}(\xi^j_k)} \tag{15}$$

with $\mathcal{L}(\xi^j_k) = \left((2\pi)^n \sqrt{|\mathbf{S}_k|}\right)^{-1} e^{-0.5 \bar{\epsilon}^{jT} {\mathbf{S}_k}^{-1} \bar{\epsilon}^j}$. The particle approximations for the parameters and states are then estimated as:

$$\mathbf{x}_{k|k} = \sum_{j=1}^{N} w(\xi^j_k)\mathbf{x}^j_{k|k}; \quad \text{and} \quad \theta_{k|k} = \sum_{j=1}^{N} w(\xi^j_k)\xi^j_k \tag{16}$$

5 Numerical Experiment

The proposed SHM approach has been tested on a simplex tensegrity. Simplex tensegrities (see Fig. 2) are a type of cylindrical tensegrity with 3 bars and 9 cables. For dynamic analysis, it is fixed at its bottom nodes (1-3) while ambient Gaussian force is applied in x-dir on the fourth node (see Fig. 2). 90% damage is induced in element 11 (bar) of the simplex. Nine strain gauges are attached on all the unrestricted members, i.e, elements 4-12, from where the measurements are collected.

The initial statically stable coordinates (see Fig. 2) are obtained from [10]. The stable form of the simplex is further excited with an ambient WGN forcing of variance $10^4 N$ throughout the simulation. Damage is initiated 0.5 s after the start of the simulation. The response from strain gauges is sampled at a fixed sampling frequency of 100 Hz for 5 seconds and further contaminated with a WGN of 1% SNR.

The initial distribution type for the parameter particles (health indices) is set to be Gaussian, with their mean set as 1 assuming an undamaged condition and a

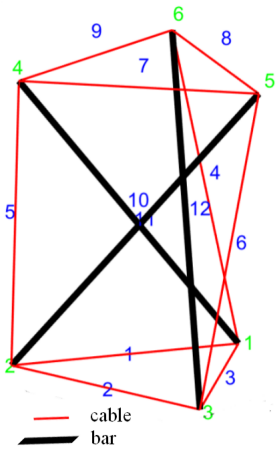

Node	X	Y	Z
1	577.4	0	0
2	-244.4	500	0
3	-266.5	-461.7	0
4	-452.3	301.5	919.4
5	9.4	-542.4	919.4
6	509.4	279.3	919.4

Fig. 2: Simplex Tensegrity Configuration

standard deviation of 0.02. 2500 filter particles are selected for PF while 75 ensembles are chosen for EnKF. A better precision may however be expected with a higher number of particles or ensemble in exchange of a higher computational cost.

Fig. 3 compares the effect of various SNR (1%,2% and 5%) on the proposed approach for simplex. It can be observed that the damage percentage estimated is fairly precise and prompt for all the SNR levels, but the promptness of detection is rather poor for 5% SNR. This, however, can be improved at higher computational cost. The method is observed to perform poorly for 10% SNR levels which demarcates the limitation of the approach.

6 Conclusion

A novel interacting filtering based damage detection technique has been proposed for tensegrity structures. EnKF is coupled with PF for simultaneous estimate of system states along with identification of a set of location based health parameters that monitor the stiffness deterioration. The health assessment is performed using ambient vibration response without knowing the input forces explicitly. The proposed method is found to be prompt and precise in detecting damages in a simplex tensegrity. The sensitivity of the proposed method under different SNR levels (1%.2%,5% and 10%) has been investigated and limiting SNR level (10%) is also identified.

Funding: This study was funded by Science & Engineering Research Board (SERB), New Delhi, India, through grant file no. ECR/2018/001464.

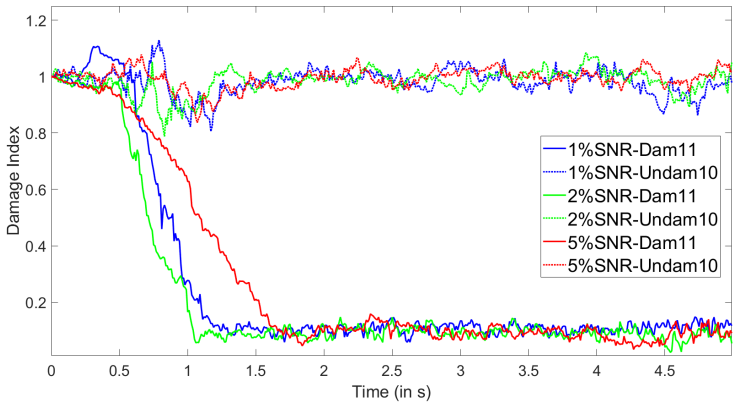

Fig. 3: Measurement noise sensitivity of proposed approach for simplex tensegrity

References

1. N. Ashwear and A. Eriksson, "Natural frequencies describe the pre-stress in tensegrity structures," *Computers & Structures*, vol. 138, pp. 162–171, 2014.
2. A. Sabouni-Zawadzka, W. Gilewski, *et al.*, "Inherent properties of smart tensegrity structures," *Applied Sciences*, vol. 8, no. 5, p. 787, 2018.
3. S. Bhalla, R. Panigrahi, and A. Gupta, "Damage assessment of tensegrity structures using piezo transducers," *Meccanica*, vol. 48, no. 6, pp. 1465–1478, 2013.
4. A. C. Sychterz and I. F. Smith, "Using dynamic measurements to detect and locate ruptured cables on a tensegrity structure," *Engineering Structures*, vol. 173, pp. 631–642, 2018.
5. R. Ghanem and G. Ferro, "Health monitoring for strongly non-linear systems using the ensemble kalman filter," *Structural Control and Health Monitoring: The Official Journal of the International Association for Structural Control and Monitoring and of the European Association for the Control of Structures*, vol. 13, no. 1, pp. 245–259, 2006.
6. K. Kebiche, M. Kazi-Aoual, and R. Motro, "Geometrical non-linear analysis of tensegrity systems," *Engineering structures*, vol. 21, no. 9, pp. 864–876, 1999.
7. A. K. Chopra, *Dynamics of structures, a primer*, vol. 2. Earthquake Engineering Research, 1995.
8. S. Sen, A. Crinière, L. Mevel, F. Cérou, and J. Dumoulin, "Seismic-induced damage detection through parallel force and parameter estimation using an improved interacting particle-kalman filter," *Mechanical Systems and Signal Processing*, vol. 110, pp. 231–247, 2018.
9. G. Evensen, "The ensemble kalman filter: Theoretical formulation and practical implementation," *Ocean dynamics*, vol. 53, no. 4, pp. 343–367, 2003.
10. M. Attig, M. Abdelghani, and N. b. Kahla, "Output-only modal identification of tensegrity structures," *Engineering Structures and Technologies*, vol. 8, no. 2, pp. 52–64, 2016.